Microfibrillar reinforced composite from drawn poly(ethylene terephthalate)/ nylon-6 blend

S. Fakirov and M. Evstatiev
Laboratory on Structure and Properties of Polymers, Sofia University, 1126 Sofia, Bulgaria

and J. M. Schultz*
Materials Science Program, Spencer Laboratory, University of Delaware, Newark, DE 19716, USA
(Received 6 July 1992; revised 3 March 1992)

Homopolymer poly(ethylene terephthalate) (PET) and nylon-6 (PA-6) and a blend (1:1 by weight) of these polymers, are each extruded as strips and ultraquenched from the melt. After zone drawing and additional annealing at temperatures, T_a, of 220 or 240°C for 5 or 25 h in vacuum, the samples are studied by differential scanning calorimetry, small-angle and wide-angle X-ray scattering, and mechanical testing. It is found that all components in the blend are oriented and that the perfection of the structure develops with increasing T_a up to 220°C. At $T_a = 240$°C, isotropization of the PA-6 component is observed, while the orientation of the PET is preserved. A microfibrillar reinforced composite is obtained, with mechanical properties as high as those of glass-fibre-reinforced nylons and surprisingly large (about 100 ×) deformability. It is shown that during thermal treatment for longer time, in addition to physical processes (crystallization and relaxation), chemical interactions (additional condensation and exchange reactions) take place at the interfaces, resulting in the formation of PET–PA-6 block copolymers playing the role of compatibilizers. Further interaction between PET (partially) and PA-6 (completely) amorphous phases leads ultimately to the involvement of the entire amount of PA-6 in the block copolymers, thus converting the starting PA-6 matrix of the microfibrillar reinforced composite into a PET–PA-6 copolymer matrix.

(Keywords: microfibrillar reinforcement; composites; blends)

INTRODUCTION

Reports on the relation between the structure, compatibility and properties of blends of semicrystalline and/or amorphous polycondensates (polyamides and polyesters) have appeared recently in the literature[1–9]. Direct relations between properties, on the one hand, and compatibility and morphology, on the other, have been established. Furthermore, the morphology and compatibility depend strongly on the nature (physical and chemical) of homopolymers, as well as on the blending conditions. Since polymers are most often incompatible, considerable efforts are directed to the improvement of compatibility or to the suppression of incompatibility. One of the approaches to the solution of this problem makes use of the peculiarities in the chemical nature of thermoplastic polycondensation polymers, i.e. the presence of reactive end carboxy, amine, hydroxy and other groups, as well as of groups resulting from their interactions. Thus a possibility exists for the occurrence of either exchange or condensation reactions, with the copolycondensates formed at the interface playing the role of compatibilizers of the homopolymers. Such effects can influence the morphology as well.

The structure–property relations in blends of linear polycondensates are studied mainly in the isotropic state[1–9]. However, a previous investigation of ours[10] showed that a certain specificity exists in the formation and type of supermolecular organization in two- and three-component blends of poly(ethylene terephthalate) (PET), nylon-6 (PA-6) and poly(butylene terephthalate) (PBT) subjected to drawing and annealing at different temperatures, T_a. It is found that all components in the blend are oriented and that the perfection of the structure improves with increasing T_a up to 220°C. In the blend at $T_a = 240$°C, isotropization of PA-6 is observed, with preservation of the orientation of PET; a microfibrillar-reinforced composite is obtained with improved mechanical properties as compared to undrawn PA-6.

The aim of the present study is to follow and distinguish between the contributions of physical and chemical processes to the structure and properties of a zone-annealed and additionally thermally treated PET/PA-6 blend. Taking into account the great commercial importance of these polymers when produced on a large scale (mainly for the manufacture of fibres and films), this investigation could be of sound practical importance in the preparation of hybrid films and fibres with new or improved properties.

* To whom correspondence should be addressed

0032-3861/93/224669-11

EXPERIMENTAL

The polymers used were PET (Goodyear Merge 1934F, $M_n = 23\,400$) and PA-6 (Allied-Signal Capron 8200, $M_n = 20\,600$). These polymers were ground to a particle size of less than 0.4 mm (after cooling in liquid nitrogen) and then mixed in the solid state (1:1 w/w). Films of this blend and of the respective homopolymers were prepared according to the following procedure. A capillary rheometer, flushed with argon and heated to about 280°C, was loaded with powdered material. The melt obtained was kept in the rheometer for 5–6 min and then extruded through the capillary (1 mm diameter) on metal rolls rotating at about 30 rev min^{-1}. The rolls were immersed in a quenching bath of liquid nitrogen. In this way, films of both homopolymers and the blend were prepared, their thickness (0.10–0.13 mm) and width (4–5 mm) depending on the extrusion rate and distance between the rolls.

It was established by X-ray and calorimetric studies that, immediately after quenching, PET was completely amorphous while the films of PA-6 and the PET/PA-6 blend (sample B) were partially crystalline.

All films were oriented according to the method of zone drawing[11,12] under the following conditions: the zone drawing was performed on the as-quenched films by moving a specially designed heater (a narrow cylindrical element, diameter 2 mm), attached to the crosshead of a Zwick tensile testing machine, from the lower to the upper part of the samples under tension. The heater was moved at 10 mm min^{-1}. A tension of 15 MPa was applied to the films. The temperature of the heater was 85°C for PET and 180°C for PA-6 and the PET/PA-6 blend. The zone-drawn films were subsequently annealed in vacuum with fixed ends at 220 or 240°C for 5 or 25 h. The sample preparation conditions are given in *Table 1*.

Differential scanning calorimetry (d.s.c.) measurements of all samples were carried out on a Perkin–Elmer 2C thermoanalyser at a heating and cooling rate of 10°C min^{-1}. After keeping the sample at a maximum temperature of 290°C for 1 min, non-isothermal crystallization from the melt was performed. The samples thus crystallized, having different thermal prehistory, were subjected to a second melting.

Table 1 Sample preparation conditions

Sample	Zone-drawing temperature[a] (°C)	λ	Annealing in vacuum with fixed ends: T_a (°C)	t_a (h)
PA, as quenched	–	–	–	–
PA-I	180	3.8	–	–
PA-I-1	180	3.8	220	5
PA-I-2	180	3.8	220	25
PET, as quenched	–	–	–	–
PET-I	85	4.0	–	–
PET-I-1	85	4.0	220	5
PET-I-2	85	4.0	220	25
PET-I-4	85	4.0	240	25
PET/PA-6 blend (1:1 by weight)				
B, as quenched	–	–	–	–
B-I	180	4.2	–	–
B-I-1	180	4.2	220	5
B-I-2	180	4.2	220	25
B-I-3	180	4.2	240	5
B-I-4	180	4.2	240	25
B-I-3-I as B-I-3 drawn additionally up to $\tau = 120\%$				

[a] All samples were annealed at the moving speed of the heater, 10 mm min^{-1}; tension applied, 15 MPa

The degree of crystallinity was determined from calorimetric data (w_c(d.s.c.)) according to the equation

$$w_c(\text{d.s.c.}) = (\Delta H_f - \Delta H_c)/F\Delta H^\circ$$

where ΔH_f and ΔH_c are the heats of melting and cold crystallization, respectively, during the same heating run, F is the weight fraction of the homopolymers in the blend (in the present case 0.5) and $\Delta H^\circ = 230$ kJ kg^{-1} and $\Delta H^\circ = 140$ kJ kg^{-1} are the ideal heats of melting of PA-6[13] and PET[14], respectively.

Using a Siemens diffractometer with Ni-filtered CuKα radiation, wide-angle X-ray scattering (WAXS) transmission patterns as well as equatorial and meridional diffractograms were obtained for all drawn and annealed blends. 2θ scans from 10 to 40° were made. Using the Scherrer formula[15]

$$D = 1.07\lambda/\beta \cos\theta$$

where λ is the wavelength (1.54 Å), θ is the diffraction angle and β is the width of the reflection at half maximum, the PA-6 crystallite size was determined from the (200) reflection, while the thickness of the PET crystallites in the axial direction was assessed from the meridional scan of the ($\bar{1}05$) reflection; their size in the lateral direction was determined from the equatorial scan of the (100) reflection.

The X-ray data were also used to estimate the degree of crystallinity. To determine relative crystallinity, w_c(WAXS), a rather standard procedure was used, according to which the amorphous peak (the shape of which is determined by the WAXS pattern of as-quenched PET) is fitted to the diffraction curve so that it intersects at some points near its maximum with crystalline minima; the area under the amorphous curve is subtracted from the total diffraction pattern to yield I_c, the portion of the diffraction attributable to the crystalline regions. w_c(WAXS) is then the ratio of the integrated area under the crystalline peaks to the total integrated area I_t under the WAXS scan ($\Sigma I_c/\Sigma I_t$). No attempt was made to separate PET and PA-6 amorphous contributions.

Using a Kratky camera, small-angle X-ray scattering (SAXS) curves of the homopolymers and blends with different thermal prehistory were recorded, from which the long spacing L was estimated.

Mechanical tests were carried out at room temperature and at a crosshead speed of 5 mm min^{-1} using a Zwick 1464 tensile tester equipped with an incremental extensiometer. Young's modulus (E, in the deformation range from 0.05 to 0.5%) and tensile strength (σ) were determined from the load–extension curves, as was the relative deformation at break (ε_b). All values are averaged from five measurements.

Attempts were made to prepare 1% solutions of the samples in boiling trifluoroacetic acid for n.m.r. measurements. It was established, however, that the drawn and annealed blend is almost insoluble, while the isotropic and zone-drawn unannealed blends are completely soluble in this solvent.

RESULTS

Thermal behaviour

Curves of melting (solid lines (a)) and of non-isothermal crystallization from the melt (dashed lines (b))

of rapidly quenched, zone-drawn and additionally annealed films of PET, PA-6 and their blend (1:1 by weight) are shown in *Figures 1–5*. The melting curves of rapidly quenched samples (*Figure 1*) show glass transitions (T_g) at about 72°C for PET, 55°C for PA-6 and 64°C for the blend. The fact that the blend has a T_g value between those of the homopolymers indicates that at least a part of the amorphous portions of the two homopolymers are miscible, or are brought into a more or less homogeneous state in the melt. It should be noted, however, that this miscibility is realized here with two completely incompatible polymers having different morphology — PET, which is completely amorphous after the ultraquenching (as indicated by the quite clearly expressed peak of the subsequent cold crystallization), and partially crystalline PA-6 (as indicated by the absence of such a peak, *Figure 1a*, sample B). It is seen in *Figure 1a* that pure PET and PA-6 have one melting peak while there are three in the blend; the two peaks at higher temperatures coincide almost completely with T_m^{PA-6} and T_m^{PET} of the homopolymers. The general trend of the melting curve of the blend suggests a metastable state of this system undergoing considerable changes during heating. The d.s.c. scan shows sequentially, relaxation, crystallization, melting and recrystallization, and melting of portions of the system.

The non-isothermal crystallization calorimetry of these materials is shown in *Figure 1b*. The effect of alloying with PA-6 is to hinder the crystallization of PET. This is demonstrated in the lower PET crystallization temperature in the blend, relative to the homopolymer.

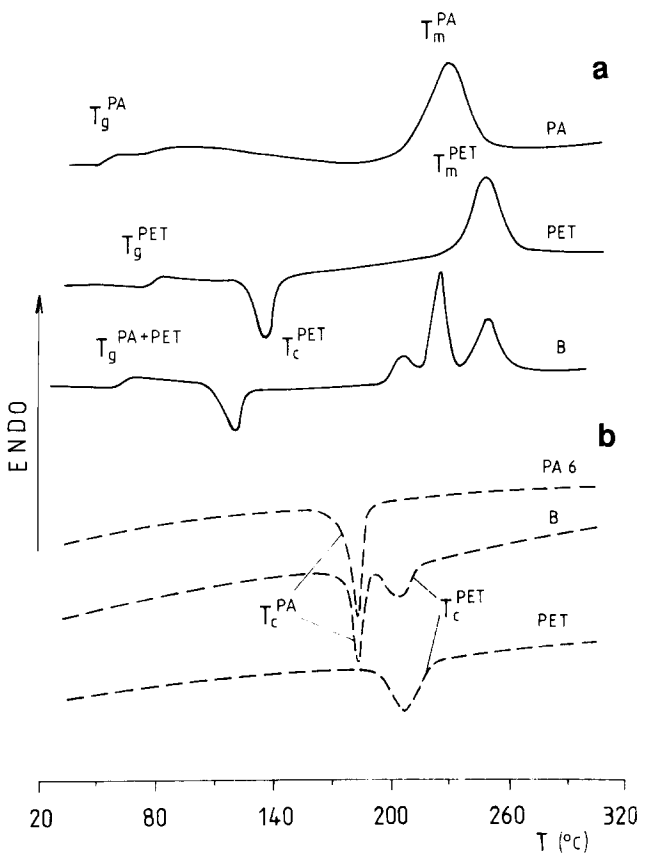

Figure 1 D.s.c. curves of ultraquenched homopolymers PET and PA-6, and of their blend (1:1 by weight) taken during: (a) first heating mode (solid lines) and (b) cooling mode (broken lines) after keeping the melt at 290°C for 1 min. For sample designation see *Table 1*

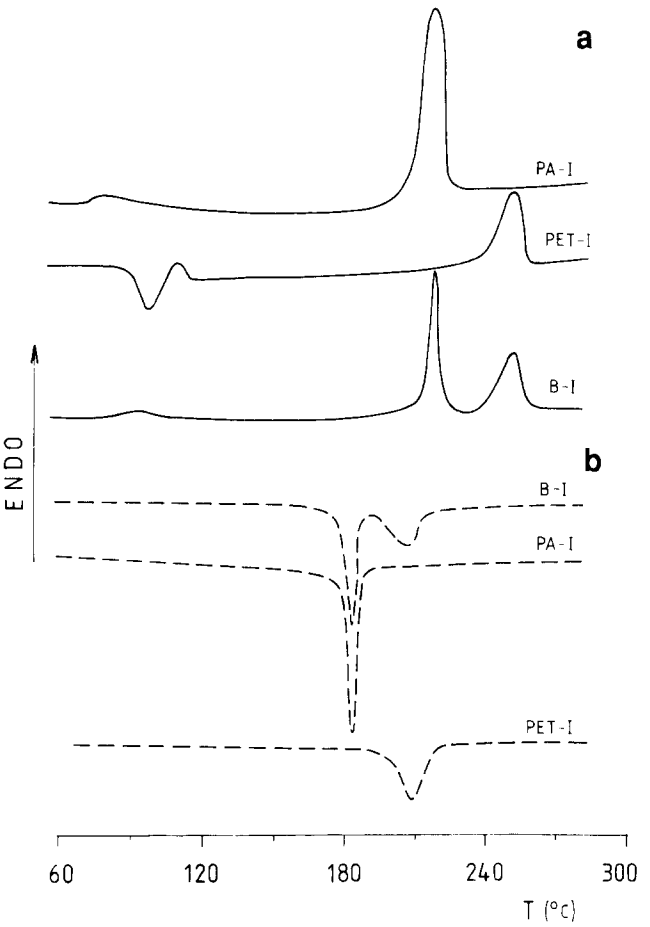

Figure 2 D.s.c. curves of same samples as in *Figure 1*, but the samples are zone drawn

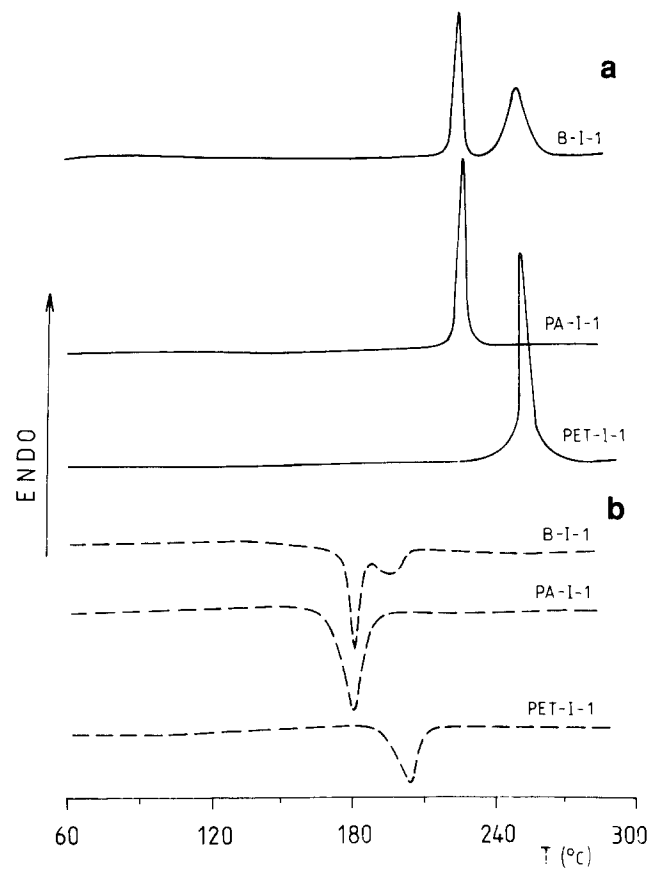

Figure 3 D.s.c. curves of same samples as in *Figure 2*, but the samples are additionally annealed with fixed ends at 220°C for 5 h

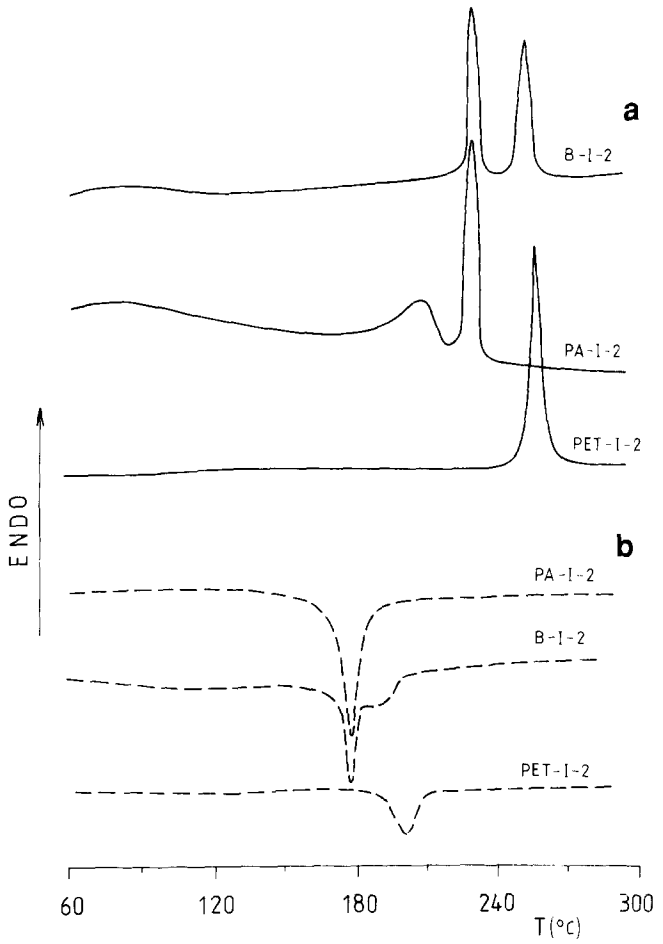

Figure 4 D.s.c. curves of same samples as in *Figure 2*, but the samples are additionally annealed with fixed ends at 220°C for 25 h

Once the PET has crystallized, the PA-6 crystallizes without hindrance. Presumably the presence of some mutual solubility of PET and PA-6 has influenced the crystallization kinetics of PET. On the other hand, once the PET species has crystallized, the remaining melt is homopolymer PA-6 and behaves as such.

Figure 2 shows thermograms of zone-drawn, unannealed PET, PA-6 and their blend (sample B-I). Both pure PA-6 and the blend again reveal one T_g which is higher by about 20°C than that of the ultraquenched samples (*Table 2*). The presence of T_g^{PA+PET} suggests the preservation of the homogeneous blend of the two polymers, while the shift of T_g to higher temperatures is a result of the decreased mobility of the chains (*Figure 2a*) due to orientation and, more importantly, to the well known effect on T_g of the crystalline phase. The trend of the melting curve of pure PET (*Figure 2a*, sample PET-I) shows a strongly expressed exotherm at about 100°C followed by an endotherm at 110°C. The lower cold crystallization temperature T_c^{PET} (*Figure 2a*), relative to that of the undrawn sample (*Figure 1a*), could be attributed to the high anisotropy of the drawn polymer, while the quite slight low-temperature endotherm could be attributed to melting of small and very imperfect crystallites arising during the previous crystallization under very unfavourable conditions. A similar trend was observed in a previous study with 20× cold-drawn PET films[16]. Again, d.s.c. scans during cooling show that the crystallization of PET is inhibited by the presence of PA-6.

The thermograms of *Figure 3* show that additional thermal treatment of the drawn samples at 220°C for 5 h leads to a sharpening of the melting peaks and to a modest increase in T_m of the homopolymers and of these components in the blend. The same trend of increase of the crystalline phase and its perfection in pure polymers and in their fractions in the blend is also observed after annealing at the same temperature for 25 h (*Figure 4*). For this reason, T_g is not observed with these samples. It should be noted that while pure PA-6 has two melting peaks (at 212 and 231°C, *Figure 4a*), the PA-6 component in the blend (sample B-I-2, *Figure 4*) exhibits one very narrow and sharp peak at 228°C.

It is suggested that the lower temperature endotherm seen in homopolymer is due to the melting of narrow interlamellar crystals formed during prolonged heat treatment. At any rate, the additional time at 225°C has somehow produced a minor population of less stable crystals. The presence of PET in the blend has inhibited this process.

D.s.c. curves of samples B-I-3 and B-I-4 blends annealed at 240°C for 5 and 25 h, respectively, are shown in *Figure 5*. It should be noted that 240°C is above the melting temperature of PA-6. Under these conditions, the PET melting endotherm remains sharp and occurs at a temperature higher than those shown in the blends of *Figures 1–4*. On the other hand, the PA-6 melting endotherm has broadened after 5 h at this temperature and occurs at a relatively low temperature (~214°C).

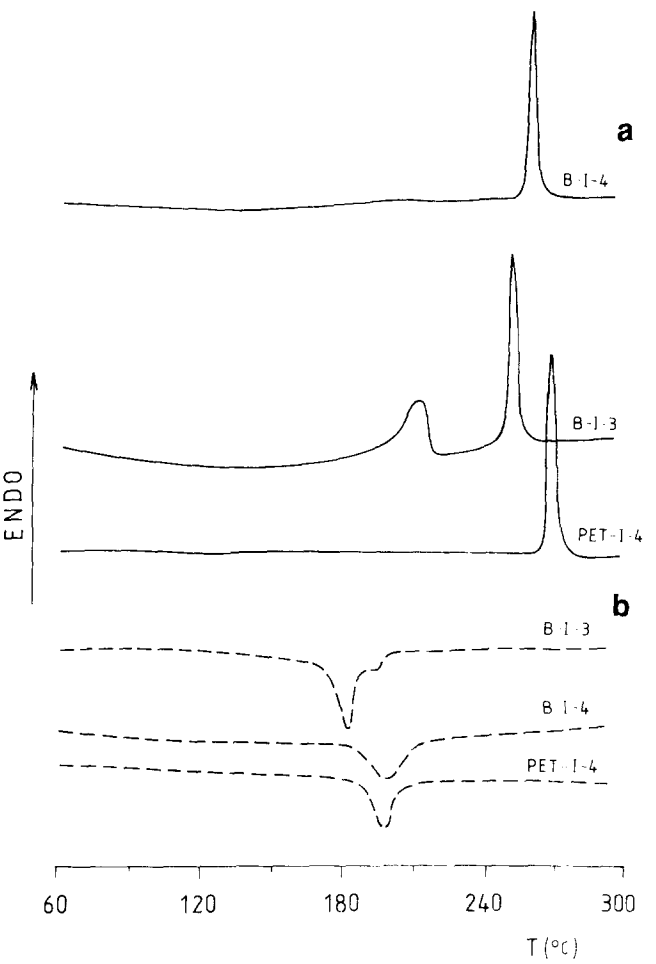

Figure 5 D.s.c. curves of same samples as in *Figure 2*, but the samples are additionally annealed with fixed ends at 240°C for 5 or 25 h

Table 2 D.s.c. data from first heating, crystallization from the melt and second heating of quenched, zone-drawn and annealed pure PET, PA-6 and PET/PA-6 blend (1:1 by weight)

Sample	First heating						Crystallization from the melt		Second heating	
	T_g (°C)	T_c (°C)	T_m (°C)	ΔH_f^a (kJ kg^{-1})	$\Delta H_f'$ (kJ kg^{-1})	$\varepsilon w_c'$(d.s.c.)^a	T_c (°C)	ΔH_c (kJ kg^{-1})	T_m (°C)	$\Sigma\Delta H_f''$ (kJ kg^{-1})
PET	72	135	254		56	0.04	204	42		
PET-I	–	104	255		58	0.10	208	44		
PET-I-1	–	–	258		74	0.51	205	36		
PET-I-2	–	–	260		71	0.49	203	34		
PET-I-4	–	–	270		69	0.48	201	28		
PA	55	–	219		64	0.28	184	52		
PA-I	76	–	218		75	0.32	185	56		
PA-I-1	–	–	229		81	0.35	185	49		
PA-I-2	–	–	212+231		72	0.31	184	50		

			PET	PA	PET	PA	$\Sigma\Delta H_f'$ (kJ kg^{-1})	PET	PA	PET	PA	$\Sigma\Delta H_c$ (kJ kg^{-1})	PET	PA	
B	64	120	254	219	53	62	58	0.17	0.25	204	184	46	255	220	45
B-I	87	–	253	220	55	68	62	0.39	0.29	206	183	43	254	219	46
B-I-1	–	–	253	227	64	88	76	0.46	0.38	194	182	39	246	214	35
B-I-2	–	–	252	228	67	83	74	0.48	0.36	190	183	40	243	212	33
B-I-3	–	–	254	214	76	44	60	0.53	0.19	192	182	36	254	211	31
B-I-4	–	–	258	–	106	–	53	0.75	–	202	–	32	249	–	26

[a] Corrected per gram of homopolymer in the blend

After 25 h, the PA-6 endotherm is very broad, of very small area and occurs at still lower temperature.

Data obtained from the d.s.c. curves of the first heating of isotropic, zone-drawn and annealed films of PET, PA-6 and their blend are summarized in *Table 2*. It is seen that the calculated enthalpy of the first melting ($\Delta H_f'$) and the degree of crystallinity w_c'(d.s.c.) per gram of homopolymer slightly increase after the zone drawing for both components. Subsequent annealing of the blend at 220°C (samples B-I-1 and B-I-2, *Table 2*) leads to a more pronounced increase in the crystallinity of both components, while their w_c' values are almost identical to those of pure polymers annealed under the same conditions. A strong decrease in the crystallinity of the PA-6 fraction (from 36 to 19%) and an increase of w_c' for the PET fraction are established after annealing for 5 h at 240°C (sample B-I-3, *Table 2*). After annealing for 25 h at the same temperature, the crystalline phase of the polyamide fraction becomes so small that it cannot be measured, while the crystallinity of the PET fraction attains its maximum value of 75% (sample B-I-4, *Table 2*). However, the sum of the enthalpies of the first melting of both components in the blend ($\varepsilon\Delta H_f'$) and hence the overall degree of crystallinity of the sample annealed at 240°C for 25 h (sample B-I-4) are lower by 40% than those of the samples annealed at 220°C (samples B-I-1 and B-I-2, *Table 2*). It is seen that annealing temperatures higher than T_m of PA-6 result in the decrease and disappearance of polyamide crystallinity and in the strong drop in the overall crystallinity. The reasons for this observation will be discussed later.

Let us now consider the non-isothermal crystallization of the homopolymers and their blend after different pretreatments. It is seen in *Figures 1b* and *2b* that the temperature range and the temperature of non-isothermal crystallization from the melt (T_c) of the exotherms of the isotropic and zone-drawn homopolymers and their blend remain almost the same. However, the trend of these curves changes for additionally annealed samples. *Figures 3b*, *4b* and *5b* show that the initial temperature of crystallization and the exotherm maximum (T_c^{PET}) of the PET fraction in the blend (B-I-1, B-I-2 and B-I-3) are 10°C lower than the values for pure homopolymers (*Table 2*). However, the exotherms of the polyamide fraction are narrower and sharper than those of pure PA-6 and occur at the same crystallization temperature (*Table 2*).

The blend subjected to annealing for 25 h at 240°C lacks a crystallization peak for the PA-6 fraction (*Figure 5b*, sample B-I-4), while the PET fraction shows a very well expressed, although broader, exotherm with its maximum coinciding with T_c^{PET} of the pure polymer undergoing the same thermal treatment (*Figure 5b*, sample PET-I-4).

It is seen from *Table 2*, where the sums of the enthalpies of both fractions calculated from the curves of non-isothermal crystallization ($\Sigma\Delta H_c$) are presented, that, in a similar way to $\varepsilon\Delta H_f'$, this magnitude decreases after the first melting of the blend with increasing annealing temperature and duration (from sample B-I-1 to sample B-I-4). It should be noted, however, that while the polyamide fraction is the basic contributor to the $\Sigma\Delta H_c$ values of samples B to B-I-3, the magnitude of $\Sigma\Delta H_c$ in sample B-I-4 is due solely to the PET fraction in the blend (*Figure 5b*) and this is about 20% higher than that of the pure polymer (sample PET-I-4, *Table 2*). A similar increase of the PET crystallinity after crystallization from the melt of PET/amorphous (non-crystallizable) polyamide blends has already been reported[9].

Figure 6 shows curves of the second melting of blends crystallized from the melt after the first melting of isotropic material and after zone drawing and

annealing at different temperatures. It is seen that the melting temperatures of both components in the annealed samples are considerably lower than the melting temperatures of the same fractions after the first melting (*Figures 3*, *4* and *5*). This is due to the isotropization of the two components of the blend after the first melting. It is also seen in *Figure 6* that sample B-I-4 again lacks a melting peak for the PA-6 fraction, while the PET fraction shows a fairly well expressed peak with enthalpy completely forming the heat of melting of the system. In *Table 2*, where the sums of the enthalpies after the second melting are presented, it can be seen that $\Sigma\Delta H_f''$ decreases with increasing annealing temperature and duration, from sample B to sample B-I-4. A crystallization peak was not observed with all samples; this means that the two homopolymers have crystallized completely during the previous cooling of their melts at a rate of 10°C min^{-1} (*Figure 6*).

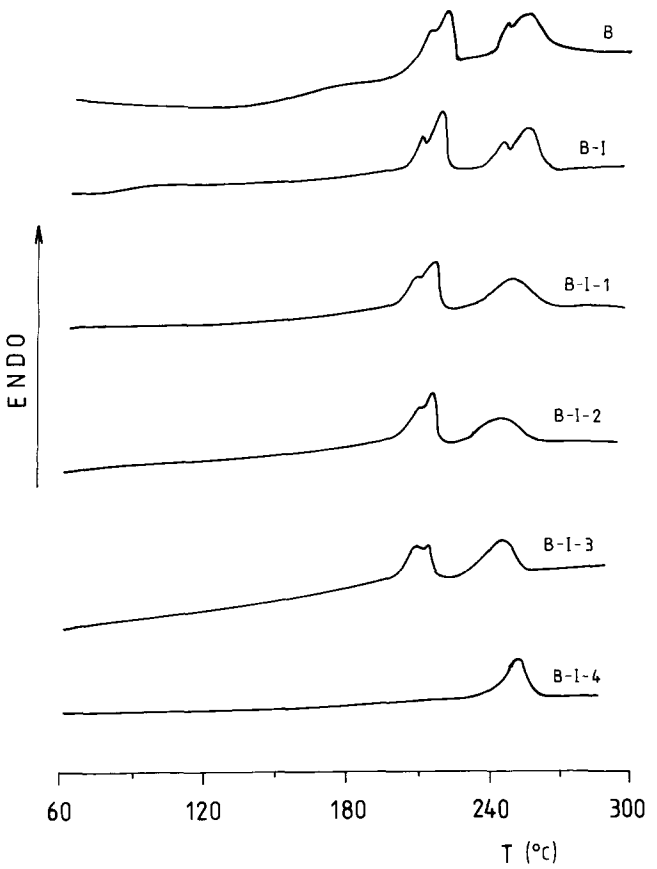

Figure 6 D.s.c. curves of PET/PA-6 blend (ultraquenched, zone drawn and additionally annealed at different temperatures and durations) taken in second heating mode. For sample designations see *Table 1*

WAXS and SAXS measurements

WAXS transmission patterns of PET/PA-6 blend films zone drawn and then annealed at various temperatures and durations are presented in *Figure 7*. For the zone-drawn blend (B-I-1), the concentration of the amorphous halo in the equatorial direction and the breadth of the crystalline reflections suggest a very good orientation of the chains in the axial direction and the presence of small and imperfect crystallites. The disappearance of the halo and the sharpening of the reflections in the equatorial and meridional directions after additional thermal treatment at 220°C (sample B-I-1) are indications of improvement of chain orientation and perfection and/or growth of the crystallites. In the case of the sample annealed at 240°C for 5 h (B-I-3), the PA-6 diffraction is in the form of Debye rings, showing the isotropy of that component. At the same time, the orientation and perfection of the crystallites in the PET fraction remains unchanged. Prolonged annealing (25 h) at the same temperature leads to the near disappearance of the PA-6 Debye rings, as well as to an improvement of the perfection of crystallites in the PET component (sample B-I-4).

Figure 7 shows a WAXS pattern of sample B-I-3-I

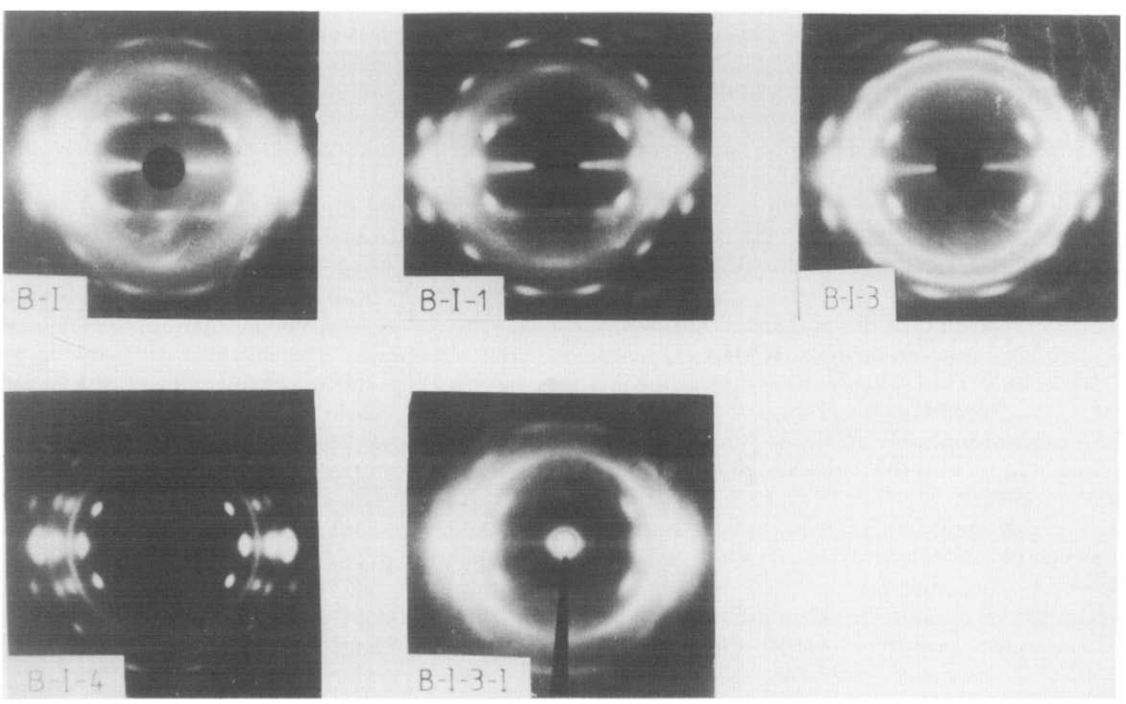

Figure 7 WAXS transmission patterns of PET/PA-6 blend, zone drawn and annealed at different temperatures. For sample designation see *Table 1*

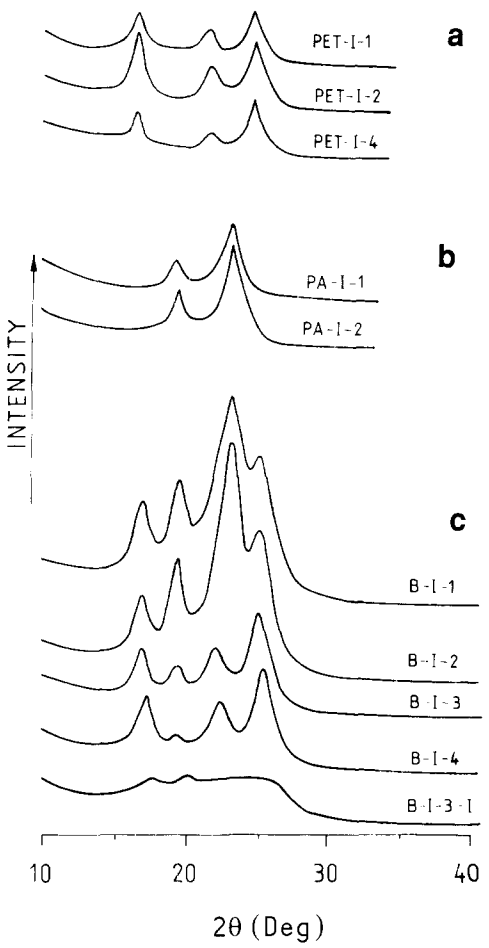

Figure 8 WAXS equatorial transmission diffractograms of PET/PA-6 blend, zone drawn and annealed at different temperatures. For sample designation see *Table 1*

obtained after additional drawing (of about 120%) at room temperature. As a result of this mechanical treatment, some orientation of the PA-6 fraction and a marked decrease in the orientation in the PET fraction are observed.

Some of the peculiarities discussed above are also noted in the diffractograms of the samples, presented in *Figure 8*. In this figure, all curves are from geometrically similar samples and are presented at the same scale, thus the intensities can be directly compared. It is seen, for all thermally treated samples, that the blend has a stronger scattering power than the homopolymers. Taking into account that the scattering power of the blend is a result of the combined effect of the two crystalline phases, these differences in the diffractograms of the homopolymers and the blend are quite natural. It should be noted, however, that the maximum integral intensity of the samples annealed at 220°C is considerably higher than that of the samples annealed at 240°C. This difference is probably due to differences in the perfection and volume fraction of the crystalline phase in the sample sets annealed at 220 and 240°C. Actually, as seen in *Table 3*, the overall degree of crystallinity (Σw_c(WAXS)) of samples B-I-3 and B-I-4 is lower by about 65% than that of the blends annealed at 220°C. The diffractograms of samples B-I-3 and B-I-4 show unambiguously that the decrease in the crystallinity in these cases is due to an abrupt drop in the crystallinity of the polyamide component of the blend. The strong decrease of the crystallinity in sample B-I-3 after additional drawing (from 29 to 19%, *Table 3*) could be attributed to chain defolding in the two components of the blend under the action of the external mechanical field (sample B-I-3-I, *Table 3*).

Data on the crystallite size are also presented in *Table 3* for all samples, using reflections appropriate for this determination. It is seen that after annealing the polyamide crystallite size increases, both in the homopolymer and in the blend. It should be noted, however, that for both components, the crystallite size in the direction perpendicular to the orientation axis in the case of homopolymers is greater by 10–20 Å than that of their respective fractions in the blend. The size determined from the ($\bar{1}05$) reflection of PET is almost the same as the lamellar thickness of pure PET and is unaffected by the annealing temperature (*Table 3*). Compared to sample B-I, a three-fold increase of the crystallite size in the polyamide fraction is observed with sample B-I-3. Due to the low intensity of the polyamide reflections, little can be inferred about crystallite sizes in the blend after annealing at 240°C.

Figures 9 and *10* show SAXS curves of isotropic, zone-drawn and annealed pure PET, PA-6 and their blend. Here, the specimens are scanned about an axis perpendicular to the drawing direction. The SAXS curves of the rapidly quenched samples have a very low intensity and no peak is observed. These experimental results are another indication of the very good blending and dispersion of the two polymers in the samples (*Figure 10*, sample B). The strong increase in the SAXS intensity after zone drawing of the blend (*Figure 10*, sample B-I) is due to the considerable increase in the overall density difference ($\Delta\rho$) between the crystallites and the amorphous phases of each component, and perhaps also between the two amorphous phases. Zone-drawn PA-6 (*Figure 9*, sample PA-I) reveals a SAXS peak, suggesting that under these conditions of drawing, sufficiently large crystallized volumes have been created. The same does not hold for PET homopolymer (*Figure 9*, sample PET-I).

Clearly expressed SAXS maxima are observed with pure polymers and their blend after additional thermal treatment of the drawn material (*Figures 9* and *10*). The large breadth of the SAXS curves could be related to the overall contribution of the alternating structures

Table 3 WAXS and SAXS data of zone-drawn and annealed pure PET, PA-6 and PET/PA-6 blend (1:1 by weight)

Sample	$D^{PET}_{(010)}$ (Å)	$D^{PET}_{(105)}$ (Å)	$D^{PA}_{(200)}$ (Å)	L (Å)	w_c(WAXS)
PET-I	–	–		–	–
PET-I-1	86	50		118	0.22
PET-I-2	93	50		123	0.28
PET-I-4	88	52		130	0.21
PA-I			41	80	–
PA-I-1			97	104	0.22
PA-I-2			106	–	0.24
					Σw_c(WAXS)
B-I	–	–	37	–	–
B-I-1	75	48	83	120	0.46
B-I-2	78	48	86	118	0.47
B-I-3	82	51	122	128	0.28
B-I-4	78	50	–	–	0.27
B-I-3-I	–	–	–	–	0.19

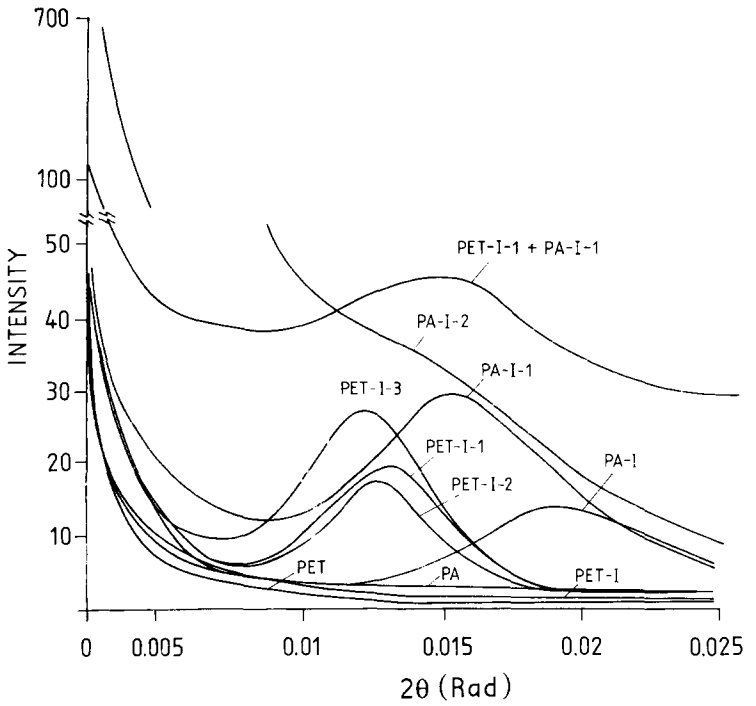

Figure 9 SAXS curves of PET and PA-6 homopolymers, isotropic, zone drawn and annealed at different temperatures and durations

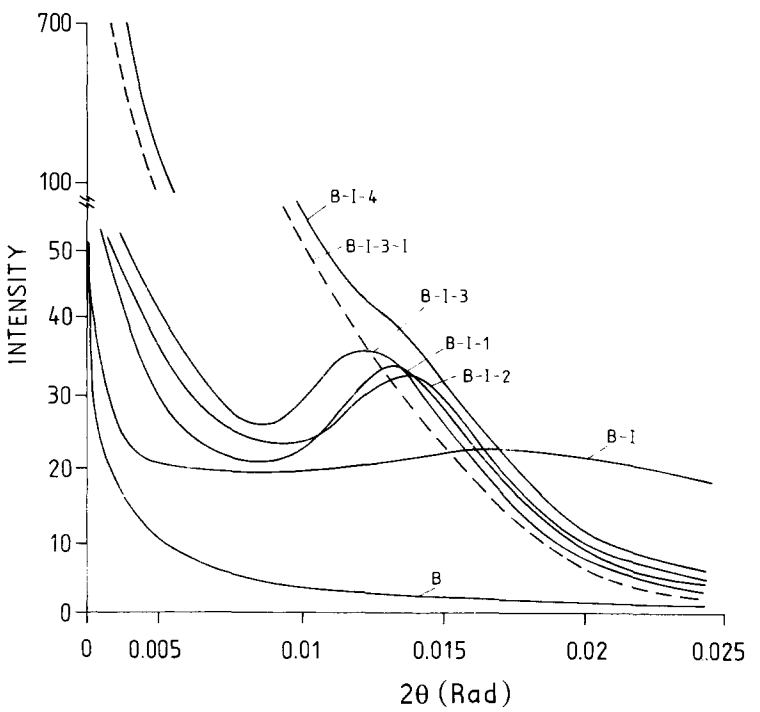

Figure 10 SAXS curves of PET/PA-6 blend (1:1 by weight), isotropic, zone drawn and annealed at different temperatures

of the two homopolymers with different but closely situated maxima, i.e. to the effect of overlapping. These assumptions find an experimental confirmation in the SAXS curve of a stack of films of pure polymers with the same thermal prehistory (PET-I-1 and PA-I-1), as shown in *Figure 9*. The maximum in the curve of this 'artificial blend' comprises the maxima of the two homopolymers, although its angular position is closer to that of fibrillized PA-I-1. Because of this overlapping, it is difficult to determine the long periods of the individual components in the blends. Only in the samples annealed for 25 h at 220°C (PA-I-2, *Figure 9*) and at 240°C, where a maximum for PA-6 is not observed, can it be assumed that the fibrillized PET is the basic structure-determining element in the annealed blends; the SAXS curves do not represent a mechanical sum of the supermolecular organization of the two homopolymers with the same thermal prehistory.

The SAXS curve of blend sample B-I-4 (annealed at 240°C for 25 h) is qualitatively different from those of all other drawn and annealed blend specimens. For B-I-4, the scattering shows a continuous decrease from $2\theta = 0$. A hump, centred near the position of the maximum for

homopolymer PET, 'rides' on this curve of continuous decrease. This type of scattering curve is predicted for imperfect stacks of crystalline lamellae[17,18] (i.e. stacks with missing lamellae) or for stacks containing very few members[19]. Simultaneous with this change in SAXS behaviour is the loss of crystalline diffraction from the PA-6 component. During the 240°C annealing treatment, the crystalline portion of the PET component is basically 'stationary', while the PA-6 melts and presumably undergoes exchange reaction with the non-crystalline PET. Since the PET degree of crystallinity has not decreased, it would appear that at least a portion of the PA-6 crystallites has been interleaved with the PET crystallites and that the non-crystalline spaces in the crystallite stacking are thus opened as the PA-6 melts, exchange chemically and cannot recrystallize upon subsequent cooling.

The SAXS curve for the annealed and redrawn material (B-I-3-I) shows only a continuously decreasing intensity about $2\theta = 0$. This is the behaviour expected of material which is so severely disrupted that no spatial correlation between crystallites remains; the crystallites scatter as isolated entities.

Mechanical properties

Some mechanical properties of zone-drawn and additionally annealed PET, PA-6 and their blend, measured under static loading conditions, are summarized in *Table 4*. Blends and homopolymers were subjected to the same processing conditions (*Table 1*), except for the zone-drawing temperature of PET films. PET films were zone drawn at 85°C, not at the standard 180°C, since at 180°C PET embrittles and breaks. It is seen that the zone-drawn homopolymers and the blend show relatively high values of Young's modulus (E) and tensile strength (σ). The values for the drawn blends are higher than the arithmetical mean of the values for the homopolymers.

After annealing at $T_a = 220$°C, the modulus slightly increases, while the strength increases in sample B-I-1 and drops slightly in sample B-I-2 (*Table 4*). After annealing for 5 h at 240°C (sample B-I-3), E and σ strongly decrease as compared to the previous samples and rise again (slightly) after annealing for 25 h at the same temperature (sample B-I-4, *Table 4*). Such a variation in the modulus and strength is also observed with the homopolymers: an increase at $T_a = 220$°C and a decrease at 240°C (*Table 4*). A considerable difference in the strain at break (ε_b) of pure polymers and their blend annealed at the same temperature is not observed. However, sample B-I-3 shows a surprisingly high deformability ($\varepsilon_b = 150\%$).

From the data on the mechanical properties of pure polymers and their blend presented in *Table 4*, it is seen that the modulus and strength of the blend do not represent a mechanical sum of their respective values in pure polymers subjected to annealing at the same temperature and duration, since the blend values are higher than the arithmetical mean values of both homopolymers.

Table 4 Mechanical data of zone-drawn and annealed pure PET, PA-6 and PET/PA-6 blend (1:1 by weight)

Sample	Young's modulus, E (GPa)	Tensile strength, τ (MPa)	Elongation at break, ε (%)
PET-I	9.4	221	9
PET-I-1	10.6	288	17
PET-I-2	11.4	316	14
PET-I-4	9.5	208	28
PA-I	4.5	342	31
PA-I-1	4.8	312	36
PA-I-2	2.7	99	56
B-I	8.8	330	36
B-I-1	9.3	346	31
B-I-2	9.8	286	29
B-I-3	7.8	159	150
B-I-4	8.6	180	21

DISCUSSION

Microfibrillar reinforcement of the blend

Zone drawing results in a high orientation of chains and of crystallites. Subsequent annealing at 220°C results in crystallite growth, an ordered stacking of crystalline lamellae and an increased degree of crystallinity. Direct transmission electron microscopy[20–28] (including work on PET, one of the homopolymers used here[26–28]) has shown that the crystallization of oriented systems begins typically with the formation of fine microfibrillar precursor crystallites with the fibrils parallel to the drawing axis. Here, the chain axis is parallel to the fibril axis. As a next stage, these systems transform into stacks of lamellar crystals, the stacking axis being parallel to the original fibrous crystallites and the chain axis still lying along the original fibril axis[28,29]. The stack can be relatively long in the stacking direction and narrow transverse to this. One can thus think of such an entity as itself a microfibril[28].

In the present case, isotropization due to melting of the PA-6 component is established at $T_a = 240$°C, the fibrillized PET preserving, however, its orientation and microfibrillar structure. As a result, a composite-like material is obtained, comprising an isotropic semicrystalline (sample B-I-3) or non-crystalline (sample B-I-4) matrix of PA-6 reinforced with semicrystalline, microfibrillized PET (*Figure 7* and *10*, *Table 3*).

The important role of the PET component in the mechanical properties is seen in *Table 4*, where some mechanical properties of the blend are reported. The blend specimens with composite-like structure (samples B-I-3 and B-I-4) show elastic moduli (Young's moduli) of 7.8 and 8.6 GPa, respectively, and tensile strengths of 159 and 180 MPa, respectively. These values are almost identical to the modulus ($E \approx 7$–8 GPa) and strength ($\sigma \approx 150$–160 MPa) of glass-fibre-reinforced (25–40% glass fibres) engineering plastic nylon 66, and are five to six times higher than those of semicrystalline isotropic polyamides ($E \approx 1$–15 GPa and $\sigma \approx 40$–50 MPa)[30]. It is useful to note that the measured modulus of these blend samples is greater than that predicted for parallel loading of the two components. Since parallel loading produces an upper bound on the modulus, it appears that blending with PA-6 induces a new microstructural state for the PET component, perhaps microfibrils with a higher aspect ratio.

The still higher values of E and σ of the blend annealed at 220°C (samples B-I-1 and B-I-2, *Table 4*) are also noteworthy. It is possible that this behaviour is due to the presence of a higher number of intra- and interfibrillar

tie molecules under stress in these samples, compared to those annealed at 240°C.

In addition to the mechanical properties, the fibrillar PET determines, to some extent, the thermophysical properties of the blends, too. This is confirmed by the absence of 'hanging down' (macroscopic melting) of the films during annealing with fixed ends, even at 240°C.

Solid-state reactions improving the homopolymer compatibility in the blend

As emphasized above, parallel to the physical changes discussed earlier, chemical interactions (solid-state exchange reactions and additional condensation) also take place in the blends at high annealing temperatures. They occur predominantly in the non-crystalline phases of the homopolymers, since these phases are characterized by: (i) enhanced molecular mobility under these conditions; (ii) relatively large interface area; and (iii) a higher number of reactive chain ends and entanglements under stress of macrochains of the two components in the drawn blend. All three of these features act to enhance the rate of exchange reaction[31–33]. The block copolymers formed through such exchange in turn influence the morphology and properties of the blend[1–9,34,35]. This interrelation provides a possibility for the indirect establishment and confirmation of the occurrence of solid-state reactions, through following the structural changes in the blend by means of typically physical parameters (T_m, T_c, W_c, solubility, mechanical properties, etc.).

The d.s.c. and WAXS data presented in *Tables 2* and *3* suggest that, regardless of the different methods of investigation, the overall degree of crystallinity (Σw_c(WAXS)) and enthalpy of melting ($\Sigma\Delta H_f'$) at the first heating, and consequently Σw_c(d.s.c.) decrease with increasing annealing temperature and duration (from sample B-I-1 to sample B-I-4). As seen in the tables and *Figures 5* and *8*, the reason for the decrease in the overall crystallinity of the blend is the diminishing contribution of the polyamide component.

These experimental results illustrate that the polyamide component loses its ability to crystallize in the blend. This loss is in turn an indication of chemical interaction and formation of a copolymer involving the entire initial amount of PA-6. Such behaviour has been observed previously: Golovoy *et al.*[34] report the non-appearance of the crystalline phase in PET upon cooling after a 30 min retention at 300°C of molten PET/polyarylate and PET/polycarbonate blends. It should be noted, however, that in the above case the chemical interactions take place in the melt, at a temperature 40°C above the melting point of the crystallizable polymer (the second component being non-crystallizable). In the case of the PET/PA-6 blend, only the polyamide component is in the molten state at 240°C, while PET retains its fibrillar microstructure (*Figure 8*). For this reason, the copolymer formed under these conditions is likely built up of short PET blocks (originating solely from the amorphous fraction of this polymer) and of relatively long PA-6 blocks (since the entire PA-6, being in the molten state, participates in the chemical reactions). The presence of longer PA-6 blocks leads to the formation, upon cooling, of small and imperfect PA-6 regions of some ordering, which follow, to some extent, the orientation of the PET component (*Figures 7* and *8*, sample B-I-4). The preservation of the ability of the PET to crystallize in sample B-I-4 is related to the retention of its fibrillar structure, i.e. to the circumstance that the chain segments building up the crystallites do not participate in chemical interactions during annealing at 240°C and thus entire macromolecules or long PET segments remain free of PA-6.

It is likely that solid-state reactions also exist at $T_a = 220$°C (near the melting point of PA-6), although to a lower extent in this case[31]. Indications of this are the broader temperature range and the lower (by about 10°C) temperatures of crystallization from the melt of the PET component in the blend, compared to those of the homopolymer with the same thermal prehistory, as well as the lower (by about 30–35%) $\Sigma\Delta H_f''$ values of samples B-I-1 and B-I-2, as compared with the heat of the second melting of thermally untreated samples (*Table 2*, samples B and B-I). The greater difference in the $\Sigma\Delta H_f''$ values (by 55–75%) of these last samples and those annealed at 240°C is evidence for the higher degree of chemical interaction in samples B-I-3 and B-I-4 as compared to those annealed at 220°C (*Table 2*).

The copolymer layers formed at the phase boundary of the two components play the role of chemical compatibilizers of the blends, similar to that of chemical coupling agents. Such agents act to improve adhesion and compatibility between fibre and polymer matrix. The presence of such copolymer layers explains why fibrillation and cleavage of the annealed blend were not observed upon the mechanical tests. Even at a deformation of about 150% of the composite-like sample B-I-3, cleavage and pull-out (pulling out of the highly oriented and fibrillar PET fraction from the isotropic PA-6 matrix) were not observed. Instead, because of the restricted deformability of the copolymeric interphase, only orientation of the isotropic matrix and disorientation of the fibrillized PET are observed under the action of an external mechanical field (*Figure 7*, sample B-I-3-I). At the same time, a partial destruction (probably by defolding) of the crystallites of the blend takes place, leading to an overall decrease in crystallinity (*Figure 8*, *Table 3*, sample B-I-3-I). The considerably lower deformations at break of the other samples of the thermally treated blend could be related to the higher anisotropy (orientation) of the two components in samples B-I-1 and B-I-2, and to the stronger interaction in the non-crystallizing block copolymer in sample B-I-4, leading also to a small increase of the modulus and tensile strength of this sample (*Table 4*).

It is important to note here that the observed compatibilizing effect resulting from the formation of copolymer layers at the interface between the two components of the blend can be effective only at the initial stages of chemical interaction. With a larger degree of exchange (through higher annealing temperature and/or annealing duration), one of the components (PA-6 in the present case) can be completely converted into a copolymer. This trend would result in the total change of the chemical composition of the microfibrillar reinforced composite, the initial matrix of homo-PA-6 being now replaced by a new one, a copolymer of PA-6 and PET. Such a change in the chemical composition of the matrix can influence the entire behaviour of the microfibrillar reinforced composite.

CONCLUSIONS

A relatively good blending of the amorphous phases of PET and PA-6 (1:1 by weight) was established in films

obtained by rapid quenching of their melt. This is confirmed by the presence of one T_g with a value between those of $T_g^{PA\text{-}6}$ and T_g^{PET}. Regardless of the substantial morphological changes occurring in the blend during the combined initial thermal and mechanical treatment (zone drawing), the blending of the two homopolymers is preserved in the anisotropic state, too. Subsequent high-temperature annealing, with fixed ends, of the drawn blend results in the parallel occurrence of physical and chemical changes. The physical changes (crystallization and relaxation) lead to an increase in size, perfection and volume fraction of the crystallites, as well as to the formation of a microfibrillar structure in the homopolymers; when annealing is carried out above $T_m^{PA\text{-}6}$ but below T_m^{PET} ($T_a = 240°C$), a composite-like structure arises. This structure comprises unoriented semicrystalline or amorphous PA-6 matrix reinforced by a semicrystalline fibrillar PET.

The chemical changes occurring in the ester–amide exchange or condensation reactions in the solid state lead to the formation of copolymer layers between the two components in the blend. This interphase plays the role of a compatibilizer. Prolonged annealing at higher temperatures (below T_m^{PET}) results in the transformation of the initially isotropic PA-6 matrix into a copolymer, which affects the morphology and properties of the blend.

ACKNOWLEDGEMENT

The authors gratefully acknowledge NSF support (Grant No. Int. 8520639). M. Evstatiev acknowledges the hospitality of the Materials Science Program at the University of Delaware, where part of this work was carried out.

REFERENCES

1 Pillon, L. Z. and Utracki, L. A. *Polym. Eng. Sci.* 1984, **24**, 1300
2 Kamal, M. R., Sahto, M. A. and Utracki, L. A. *Polym. Eng. Sci.* 1982, **22**, 1127
3 Pillon, L. Z. and Laro, J. *Polym. Eng. Sci.* 1987, **27**, 984
4 Harracher, B. D., Angeli, S. R. and Runt, J. *Polym. Bull.* 1986, **15**, 455
5 Murff, S. R., Barlow, J. W. and Paul, D. R. *J. Appl. Polym. Sci.* 1984, **21**, 3231
6 Slagowski, E. L., Chang, E. P. and Tkacil, J. *J. Polym. Eng. Sci.* 1981, **21**, 513
7 Kimura, M. and Porter, R. S. *J. Polym. Sci., Polym. Phys. Edn* 1983, **21**, 367
8 Lin, M. F. and Wong, H. H. *J. Mater. Sci. Lett.* 1991, **10**, 569
9 Nadkarni, V. M., Shingankuli, V. L. and Jog, J. P. *J. Appl. Polym. Sci.* 1992, **46**, 339
10 Evstatiev, M. and Fakirov, S. *Polymer* 1992, **33**, 877
11 Kunugi, T., Ichjinose, C. and Suzuki, A. *J. Appl. Polym. Sci.* 1981, **31**, 429
12 Kunugi, T., Akiyama, I. and Hashimoto, M. *Polymer* 1982, **23**, 1199
13 Gogolewski, S. and Pennings, A. J. *Polymer* 1977, **18**, 654
14 Wunderlich, B. *Polym. Eng. Sci.* 1979, **18**, 431
15 Cullity, B. D. in 'Elements of X-Ray Diffraction', Addison-Wesley, Reading, MA, 1978
16 Evstatiev, M., Fakirov, S., Apostolov, A., Hristov, H. and Schultz, J. M. *Polym. Eng. Sci.* 1992, **32**, 964
17 Fischer, E. W., Martin, G., Schmidt, G. F. S. and Strobl, G. Proceedings of IUPAC Symposium, Toronto, 1968
18 Schultz, J. M., Fischer, E. W., Schaumburg, O. and Zachmann, H. A. *J. Polym. Sci., Polym. Phys. Edn* 1980, **18**, 239
19 Vignaud, R. and Schultz, J. M. *Polymer* 1986, **27**, 651
20 Petermann, J. and Gohil, R. M. *J. Mater. Sci.* 1979, **14**, 2260
21 Petermann, J. and Gohil, R. M. *J. Polym. Sci., Polym. Lett. Edn* 1980, **18**, 781
22 Petermann, J. *Makromol. Chem.* 1981, **182**, 613
23 Petermann, J., Gohil, R. M., Schultz, J. M., Hendricks, R. W. and Lin, J. S. *J. Mater. Sci.* 1981, **16**, 265
24 Rau, J., Gohil, R. M., Petermann, J. and Schultz, J. M. *Colloid Polym. Sci.* 1981, **259**, 241
25 Petermann, J., Gohil, R. M., Schultz, J. M., Hendricks, R. W. and Lin, J. S. *J. Mater. Sci.* 1981, **16**, 265
26 Murray, R., Davis, H. A. and Tucker, P. *J. Appl. Polym. Sci., Appl. Polym. Symp.* 1978, **33**, 177
27 Petermann, J. and Rieck, U. *J. Mater. Sci.* 1987, **22**, 1120
28 Chang, H., Schultz, J. M. and Gohil, R. M. *J. Macromol. Sci.–Phys.* 1993, **B32**, 99
29 Schultz, J. M. and Petermann, J. *Colloid Polym. Sci.* 1984, **262**, 294
30 Du Pont de Nemours International SA, Switzerland, Brochure E-52863, 1986
31 Fakirov, S. in 'Solid State Behavior of Linear Polyesters and Polyamides' (Eds J. M. Schultz and S. Fakirov), Prentice Hall, Englewood Cliffs, NJ, 1990
32 Evstatiev, M. PhD Thesis, Sofia University, 1988
33 Dubner, W. S. PhD Dissertation, University of Delaware, 1990
34 Golovoy, A., Cheung, H. F., Garduner, K. R. and Rokosz, M. *Polym. Bull.* 1989, **21**, 327
35 Kimura, M., Salee, G. and Porter, R. S. *J. Appl. Polym. Sci.* 1984, **29**, 1629